

## Report

# Nitric Oxide Coordinates Cell Proliferation and Cell Movements During Early Development of *Xenopus*

**Natalia Peunova\***

**Vladimir Scheinker**

**Kandasamy Ravi**

**Grigori Enikolopov**

Cold Spring Harbor Laboratory, Cold Spring Harbor, New York USA

\*Correspondence to: Natalia Peunova; Cold Spring Harbor Laboratory; 1 Bungtown Road; PO Box 100; Cold Spring Harbor, New York 11724 USA; Tel.: 516.367.8316; Email: peunova@cshl.edu

Original manuscript submitted: 10/07/07

Manuscript accepted: 10/08/07

Previously published online as a *Cell Cycle* E-publication:  
<http://www.landesbioscience.com/journals/cc/article/5146>

## KEY WORDS

nitric oxide, planar polarity, *Xenopus*, proliferation, morphogenesis, convergent extension, Dishevelled, nitrosylation

## ABBREVIATIONS

8-Br-cGMP	8-Bromo-cyclic guanylate monophosphate
BrdU	5-Bromo-2-deoxyuridine
ETU	2-ethyl-thiopseudourea
ODQ	1H-[1,2,4]-oxadiazolo-[4,3- $\alpha$ ]-quinoxalin-1-one
D-NAME	D-nitro-arginine-methyl ester
L-NAME	L-nitro-arginine-methyl ester
SNAP	S-nitroso-N-acetyl-penicillamine
sGC	soluble guanylate cyclase
XNOS1	<i>Xenopus</i> nitric oxide synthase 1
dnXNOS1	dominant negative XNOS1

## ACKNOWLEDGEMENTS

See page 12.

## ABSTRACT

The establishment of a vertebrate body plan during embryogenesis is achieved through precise coordination of cell proliferation and morphogenetic cell movements. Here we show that nitric oxide (NO) suppresses cell division and facilitates cell movements during early development of *Xenopus*, such that inhibition of NO synthase (NOS) increases proliferation in the neuroectoderm and suppresses convergent extension in the axial mesoderm and neuroectoderm. NO controls cell division and cell movement through two separate signaling pathways. Both rely on RhoA-ROCK signaling but can be distinguished by the involvement of either guanylate cyclase or the planar cell polarity regulator Dishevelled. Through the cGMP-dependent pathway, NO suppresses cell division by negatively regulating RhoA and controlling the nuclear distribution of ROCK and p21WAF1. Through the cGMP-independent pathway, NO facilitates cell movement by regulating the intracellular distribution and level of Dishevelled and the activity of RhoA, thereby controlling the activity of ROCK and regulating actin cytoskeleton remodeling and cell polarization. Concurrent control by NO helps ensure that the crucial processes of cell proliferation and morphogenetic movements are coordinated during early development.

## INTRODUCTION

During the early steps of development, two major morphogenetic processes, cell division and cell movement, are tightly integrated. Active cell duplication is required to generate a sufficient number of cells; it must be coordinated with precise morphogenetic cell movements during gastrulation and organogenesis to build a correctly structured organ or a tissue and discoordination of these processes may lead to morphogenetic aberrations and congenital malformations (e.g., neural tube defects).<sup>1-6</sup> However, the alterations of cell shape and cytoskeleton rearrangements required for the complex choreography of moving cell sheets in the embryo may be incompatible with cell division; conversely, mitoses may disrupt the polarized cytoskeletal structures necessary for the directed migration of cells during embryogenesis. Indeed, the process of cell division disrupts the planar polarity of neuroepithelial cells which is required for the correct trajectory of movement of these cells in the developing neural tube; planar polarity has to be reestablished in the migrating cells of the neuroepithelium after each mitosis.<sup>7</sup>

The nature of the signals that coordinate cell division and cell movement during development has been elusive. Here we show that NO, a signaling molecule with both antiproliferative<sup>8-15</sup> and pro-motility<sup>16-19</sup> potential, regulates the machineries both of cell division and cell motility during *Xenopus* development. Changes in NO availability affect the two processes in a reciprocal manner: NO suppresses cell division and facilitates cell movement, whereas a deficit of NO increases cell proliferation and hinders cell movement. NO acts as a negative regulator of the RhoA-ROCK pathway: in a cGMP-dependent manner, it affects cell division by controlling the intracellular distribution of ROCK and p21WAF1; in a cGMP-independent manner it affects cell movements through interactions with the Dishevelled (Dsh) component of the planar cell polarity (PCP) pathway, S-nitrosylation of RhoA, control of ROCK activity, and remodeling of the actin cytoskeleton. These results reveal a molecular mechanism for the coordination of cell division with morphogenetic cell movements during early vertebrate development.

## MATERIALS AND METHODS

**Recombinant constructs.** XNOS1 gene (GenBank accession number AF053935) isolation was described earlier in ref. 12. The dnXNOS1 construct was prepared by deleting an Xba fragment of XNOS1 encompassing 272 carboxy-terminal amino acids covering the NADPH binding domain and cloning the resulting truncated cDNA into the pCS2 plasmid. The efficiency of XNOS1 inhibition by dnXNOS1 was evaluated after co-transfection of 293T cells with XNOS1 and dnXNOS1 DNA and assaying NOS activity in transfected cells using the arginine-citrulline conversion assay (as described Refs. 12,20). NOS activity in embryos injected with XNOS1 and dnXNOS1 mRNA was also evaluated in situ by NADPH-diaphorase reaction as described in ref. 12. dnXNOS1, XNOS1-HA, XNOS1-GFP constructs were prepared using standard molecular cloning techniques.<sup>21</sup> Dsh-myc, Dsh-GFP, and p21WAF1-myc constructs were gifts from Drs. S. Sokol, Y. Sasai, and S. Ohnuma, respectively. RNA for microinjections was prepared using mMessage mMachine kit (Ambion, Austin, TX) according to the manufacturer's manual.

**Embryo handling and microinjections.** Eggs were obtained after induced ovulation of female *Xenopus laevis* by injections of human chorionic gonadotropin. Eggs were fertilized in vitro, dejellied in 3% cysteine (pH 7.9) and reared in 0.3 MMR. Embryos were staged according to Nieukoop and Faber.<sup>22</sup>

Microinjections of embryos, placed in 3% ficoll in 0.3 MMR, was performed using a Harvard Apparatus microinjector PLI-100. 10 nl of NOS inhibitors 2-ethyl-2-thiopseudourea (ETU; 10 or 100 mM stock concentration); L-nitro-arginine-methyl ester (L-NAME; 100 or 1000 mM stock concentration), or its inactive enantiomer D-NAME, S-nitroso-N-acetyl-penicillamine (SNAP; 10 mM stock concentration), and RhoA kinase (ROCK) inhibitor Y27632 (100  $\mu$ M stock concentration), 8-Bromo-cyclic guanylate monophosphate (8-Br-cGMP; 10 mM stock concentration), or sGC inhibitor 1H-[1,2,4]-oxadiazolo-[4,3- $\alpha$ ]-quinoxalin-1-one (ODQ; 1 mM stock concentration) (all from Calbiochem, San Diego, CA), were injected into the blastocoel of stage 8 embryos. In the experiments aimed at perturbing NO signaling in dorsal structures, 1.5 ng of either XNOS1 or dnXNOS1 mRNA, along with 0.5 ng of either  $\beta$ -galactosidase or GFP mRNA (used as tracers) was injected into the two dorsal blastomeres of the four-cell embryo. To perturb NO signaling on one side of the embryo, mRNAs were injected into one blastomere of the two-cell stage embryo. Successfully injected embryos were selected for further analysis by epifluorescence of the GFP tracer under Nikon SMZ-U dissecting microscope or after staining with 5-bromo-6-chloro-3-indolyl- $\beta$ -D-galactopyranoside substrate for  $\beta$ -galactosidase (Biotium, Hayward, CA) as described in ref. 23. To access the changes in cellular organization, notochords were dissected from stage 23 embryos and stained by fluorescein-labeled concanavalin A and Topro3 (Molecular Probes, Eugene, OR).

Animal caps were prepared at the late blastula stage and cultured in 0.6 MMR.<sup>23</sup> L-NAME or D-NAME was added at concentration of 5 mM, SNAP at 200  $\mu$ M, Y27632, 8-Br-cGMP at 100  $\mu$ M, and ODQ at 10  $\mu$ M. For the animal cap elongation assay the media was supplemented with 10 ng/mL of human recombinant activin (R&D, Minneapolis, MN) or with activin along with L-NAME, SNAP, or Y27632 at the concentrations stated above. All groups were harvested and fixed in MEMFA<sup>23</sup> when untreated sibling embryos reached the late neurula stage.

**Immunocytochemistry.** For whole mount immunocytochemistry experiments animal caps were postfixed 15 min in Dent's fixative (20% DMSO, 80% Methanol),<sup>23</sup> cut into small pieces, and processed for whole mount immunocytochemistry according to the Klymkowsky's lab protocol (spot.colorado.edu/~klym/Methods/wholemount.htm). Polyclonal antibody M-19 to p21WAF1 (sk-471 from Santa-Cruz Biotechnology, Santa Cruz, CA; lot H262, gift from D. Helfman) (dilution 1:400), polyclonal antibody to Dsh (a gift from S. Sokol) (dilution 1:200), and monoclonal antibodies to ROCKI and ROCKII (Transduction Laboratories/BD Pharmingen, San Jose, CA) (dilution 1:200) were applied and were followed by secondary anti-rabbit or anti-mouse antibodies conjugated to Alexa 488 or Alexa 568 (Molecular Probes) (dilution 1:400). Falloidin-Alexa 488 was from Molecular Probes. Nuclei were stained with Topro3 or SYBR-Green (Molecular Probes). Images were collected on a Zeiss LSM510 confocal microscope.

**In situ hybridization, marker analysis.** Wholmount in situ hybridizations were carried out using the digoxigenine/alkaline phosphatase detection method (Roche Molecular Biochemicals, Mannheim, Germany) as described in ref. 23. The constructs to prepare hybridization probes were gifts from Drs. P. Krieg, Y. Sasai, and S. Sokol. For 5-bromo-2-deoxyuridine (BrdU) labeling, embryos at late neurula stage were injected with BrdU at concentration 1 mg/ml, fixed after two hours in 4% paraformaldehyde, treated with proteinase K, post fixed in Dent's fixative, and processed with FITC-conjugated anti-BrdU antibody (BD Pharmingen) as suggested by the manufacturer. Labeled embryos or explants were placed in FocusClear (Pacgen, Vancouver, Canada) to make them transparent and were imaged on confocal microscope. Stacks of 20  $\mu$ m optical sections were collected. The assessment of the changes in the cell number and statistical analysis were performed as described previously in ref. 12.

**Rho-Rhotekin pulldown assay, immunoprecipitation and Western blots.** RhoA activation assays were performed essentially as described in ref. 24. Embryos injected at blastula stage 8 with PBS, L-NAME, D-NAME or SNAP were harvested at late neurula stage and protein extracts from 20 embryos were incubated with Rhotekin-RBD Protein GST beads (Cytoskeleton, Denver, CO). Proteins bound to Rhotekin beads were resolved by SDS-PAGE and blotted onto PVDF membrane (Millipore, Bedford, MA); signals were visualized using antibody against RhoA (Santa Cruz Biotechnology) and chemiluminescence Superfemtomole kit (Pierce, Rockford, IL). Immunoprecipitations were performed using standard techniques<sup>21</sup> and proteins were analyzed using SDS-PAGE and Western blotting as above.

**Biotin switch assay.** Biotin switch assay to detect S-nitrosylation was performed essentially as described in ref. 25. We used the mouse brain microvascular endothelial cell line bend.3 (ATCC) which is known to produce higher amounts of NO, as a model system to express RhoA gene (gift from L. van Aelst, CSHL). bend.3 cells were transfected with a construct coding for RhoA tagged with the T7 epitope and harvested after 36–48 hrs. Typically, 500  $\mu$ g of cell lysates were used. First, the free thiols were blocked with methylmethanethiosulfonate (MMTS) and the nitrosylated thiols were oxidized using ascorbate and tagged simultaneously with Biotin-HPDP. Finally, biotinylated proteins were purified using NeutrAvidin-agarose beads (Pierce, Rockford, IL) and analyzed using Western blotting and antibodies to T7 epitope.

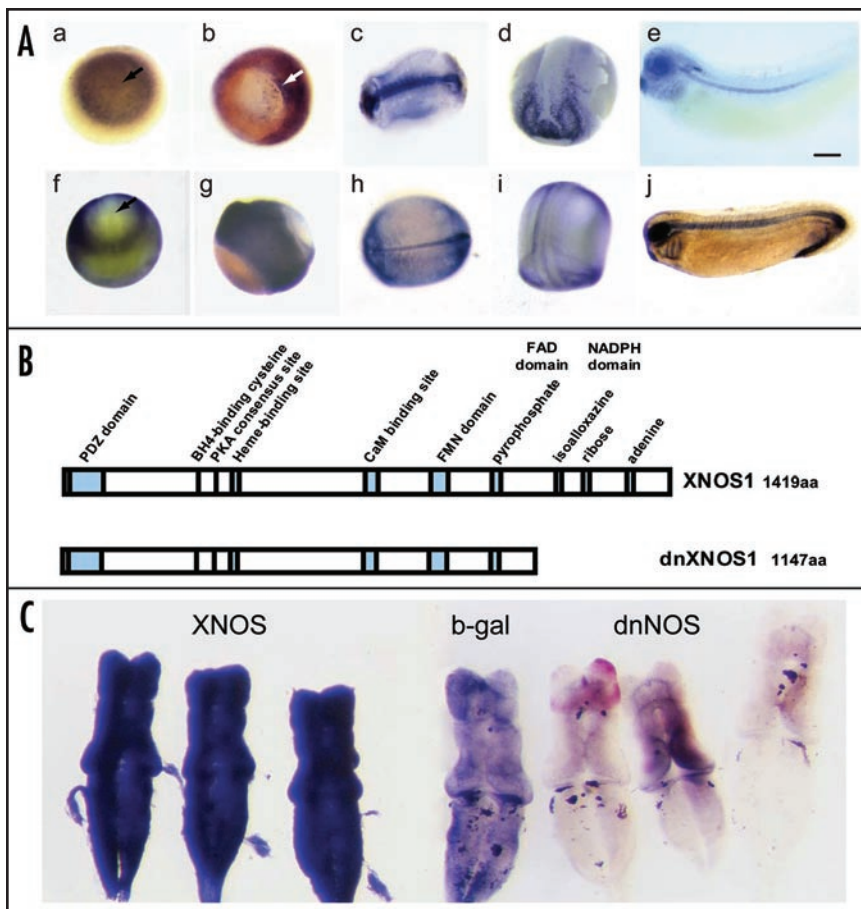


Figure 1. XNOS1 expression and activity. (A) XNOS1 is expressed during early *Xenopus* development. XNOS1 expression during early development detected by in situ hybridization (upper panel, a–e) and NADPH-diaphorase activity (lower panel, f–j): unfertilized oocytes (a and f; arrows point to the animal pole), beginning of gastrulation (b and g; arrow indicates dorsal lip), late neurula (c, d, h and i), and tadpole (e and j). Bar is 250  $\mu$ m in a–d, f–i and 500  $\mu$ m in e and j. (B) Structure of XNOS1 and dnXNOS1. XNOS1 is 1419 aa long and has all of the conserved regions of mammalian nNOS. dnXNOS1 is 1147 aa long and lacks the critical NADPH-binding domain essential for the NO synthesis. (C) Modulating NOS activity by XNOS1 and dnXNOS1. 2 blastomeres of the 2-cell embryos were injected with XNOS1,  $\beta$ -galactosidase, or dnXNOS1 mRNA. At stage 43 brains were dissected and stained for NADPH-diaphorase activity. Injection of XNOS1 mRNA increased staining (left) compared to the injection of  $\beta$ -galactosidase (center); injection of dnXNOS1 strongly decreased the staining (right).

## RESULTS

**XNOS1 regulates embryonic development of *Xenopus*.** XNOS1 is the major form of NOS found in the developing brain of *Xenopus* tadpoles.<sup>12</sup> We examined the expression of XNOS1 during early *Xenopus* development using in situ hybridization (Figs. 1Aa–e) and NADPH diaphorase staining, an indicator of NOS activity (Figs. 1Af–j). Both approaches revealed similar distribution patterns, indicating that XNOS1 accounts for most of the NOS activity during early development. XNOS1 is detected as maternal RNA and protein in the animal hemisphere of the oocyte and, after fertilization, through the blastula stages of the embryo (Fig. 1Aa and Af). At the beginning of gastrulation XNOS1 is expressed in the ectoderm and marginal zone and also in cells of the involuting mesoderm (Fig. 1Ab and Ag). In the neurula, XNOS1 is expressed in the dorsal

and lateral mesoderm and in cells lining the archenteron (Fig. 1Ac and Ah); XNOS1 expression in the ectoderm at this stage is limited to the lateral edges of the neural tube, the anterior neural ridge, prosencephalon, and the eye anlage (Fig. 1Ad and Ai). Later, in the tadpole, XNOS1 is expressed in the notochord, the eye, and the developing nervous system (Fig. 1Ae and Aj; see also ref. 12).

To experimentally increase NO production, we injected XNOS1 mRNA into one or two blastomeres of the two-cell embryo or into two dorsal blastomeres of the four-cell embryo. To decrease NO production, we similarly injected mRNA corresponding to a dominant negative version of XNOS1 (dnXNOS1, a truncated variant of XNOS1 lacking the carboxy-terminal NADPH domain; note that both XNOS1 and dnXNOS1 retain the PDZ domain) (Fig. 1B). NOS enzymes require homodimerization to be active and truncated NOS polypeptides can suppress production of NO by forming inactive heterodimers with the endogenous full length NOS polypeptide.<sup>20,26,27</sup> We used NADPH staining of embryos to assess the efficiency of modulating the NOS activity. When XNOS1 mRNA was injected, NOS activity, as judged by NADPH diaphorase staining, was strongly increased at least until stage 43 (Fig. 1C). Conversely, injection of the mRNA coding for dnXNOS1 inhibited the activity of endogenous NOS (Fig. 1C). This confirms that mRNA from recombinant variants of XNOS1 can be used to effectively up- and down-regulate NOS activity in embryos. In parallel, we manipulated NO levels by injecting either an NO donor S-nitroso-N-acetyl-penicillamine (SNAP) or NOS inhibitors L-nitro-arginine-methyl ester (L-NAME) and 2-ethyl-thiopseudourea (ETU) into the blastocoel, using the inactive enantiomer D-NAME or saline as controls.

Injections of XNOS1 mRNA or NO donor did not change the course of embryo development. In contrast, injection of the recombinant NOS inhibitor dnXNOS1 mRNA into the dorsal blastomeres had a distinct effect on the embryo morphogenesis. By the end of gastrulation (stage 12), NOS inhibition resulted in delayed (by 2–3 hours) or incomplete blastopore closure (81%, n = 210; Fig. 2A and B), and, in severe cases (~10%), resulted in failure to complete gastrulation.

By the neurula stage 19, inhibition of XNOS1 resulted in a delay in neural tube closure and a wider (and in severe cases, open), neural tube (Fig. 2Ad and Ae). Later, by the early tailbud stage (stage 23), 65% (n = 160) of the embryos displayed several types of defects: a shortened anteroposterior axis; dorsal flexure; and delayed fusion of the neural tube (Fig. 2Ag and Ah). The distortion of the streamlined shape of the embryos injected with dnXNOS1 mRNA was also apparent at later stages of development (stage 28, Fig. 2Aj and Ak and stage 43, Fig. 2Am and An). Such changes are characteristic of defects in the PCP pathway which controls cell movements during convergent extension.<sup>2,4,28</sup> Specifically, the changes induced by the NOS inhibitor resembled defects in both mesodermal convergent

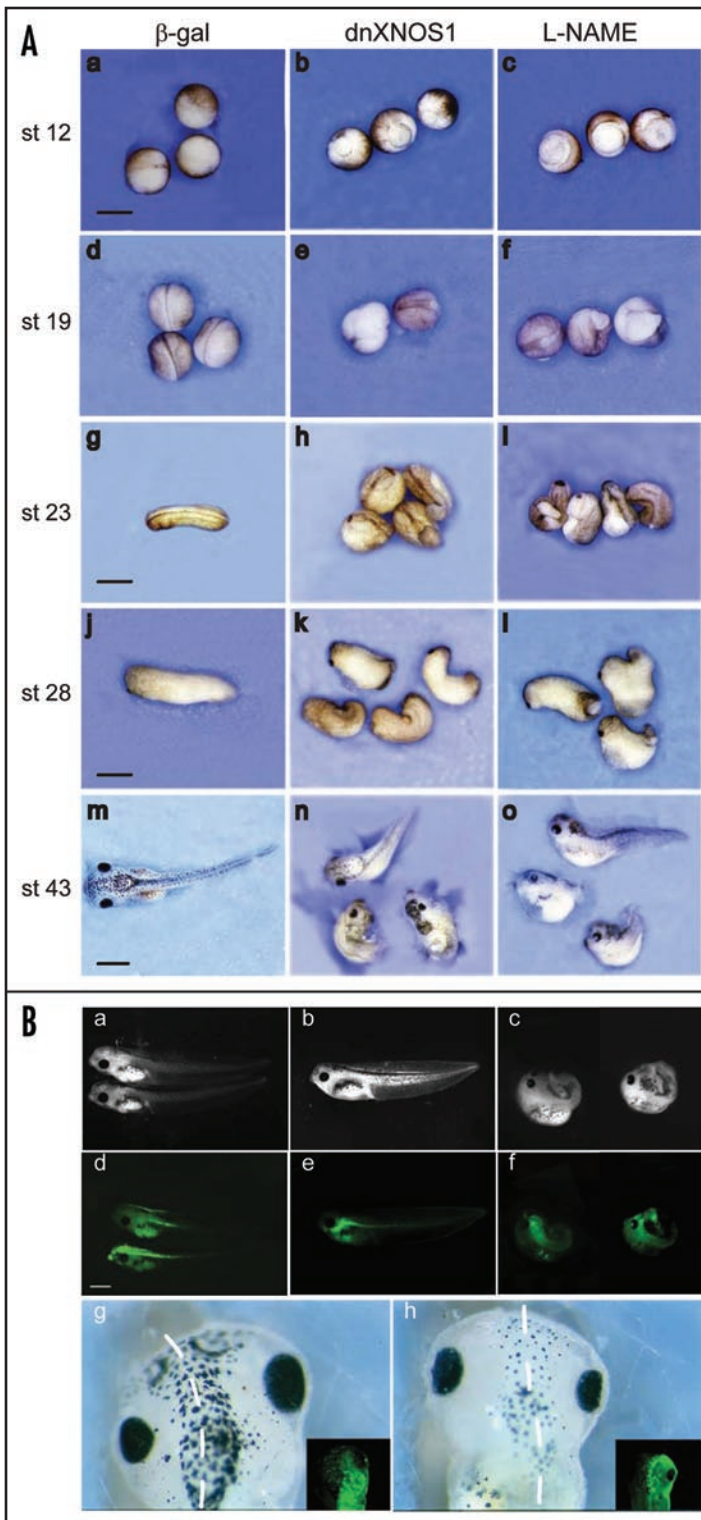


Figure 2. Inhibition of XNOS1 distorts morphogenesis and increases organ size. (A) Dorsal injections of recombinant inhibitor dnXNOS1 (b, e, h, k and n) or blastocoel injections of L-NAME (c, f, i, l and o) induce morphogenetic defects: delayed blastopore closure at the gastrula stage (b and c), a wider and incompletely closed neural tube at neurula stage (e and f), a shortened anteroposterior axis and defects in neural tube closure at the tailbud stage (h and i), and shortened axis and dorsal flexure in the tailbud and tadpole (k, l, n and o); control embryos received dorsal injections of  $\beta$ -galactosidase mRNA (a, d, g, j and m). Bar is 1 mm. (B) Targeted injections of dnXNOS1 and lineage tracing. GFP mRNA was coinjected with either  $\beta$ -galactosidase (a and d) or dnXNOS1 mRNA (b, c, e and f) into two dorsal blastomeres of the eight-cell embryo. GFP lineage tracing at stage 43 shows that delivery into the notochord is associated with shortening of the axis (b and e), whereas delivery into the nervous system is associated with dorsal flexure (c and f). In separate experiments, one blastomere of the two-cell embryos was injected with either dnXNOS1 (g) or XNOS1 mRNA (h); in both cases GFP mRNA was co-injected to trace the injected side (insets). Injection of dnXNOS1 mRNA results in a larger head and eye on the injected side, whereas injection of XNOS1 mRNA results in a smaller head and eye on the injected side.

the notochord (Fig. 2Ba,b,d and e), consistent with targeting of the mRNAs to the dorsal vegetal blastomeres and defects in mesodermal convergent extension; in turn, dorsal flexure was associated with the appearance of the GFP tracer in the neural tube (Fig. 2Bc and f), consistent with targeting of the mRNA to the dorsal animal blastomeres and defects in neural convergent extension. Together, these experiments suggest that NO is involved in controlling morphogenetic cell movements, potentially through interactions with the PCP pathway.

When dnXNOS1 was injected into the blastomeres of the two-cell embryo, the embryos underwent apparently normal axis extension. However, when we examined the embryos during organogenesis, we found that inhibition of NOS resulted in enlarged organ size in 45% ( $n = 95$ ) of the embryos. For example, injections of dnXNOS1 into one of the two blastomeres of a two-cell embryo resulted in enlarged head, brain, and eye on the injected, as compared to the contralateral, side (Fig. 2Bg).

Injection of chemical NOS inhibitors L-NAME and ETU into the blastocoel resulted in the same spectrum of phenotypes as that for the recombinant inhibitor (Fig. 2Ac,f,i,l and o). The effect of the inhibitors was concentration-dependent such that at lower concentrations (1 mM of L-NAME and 100  $\mu$ M of ETU) the predominant defect was an enlargement of the head, brain, and eye, while embryos with shortened axis and dorsal flexure were rare. At higher concentrations (10 mM of L-NAME or 1 mM of ETU) the proportion of embryos with defects in morphogenetic cell movement (shortened axis and dorsal flexure) increased to 80% (injection of the inactive enantiomer D-NAME did not affect the development of the embryos). Thus, both types of inhibitors (recombinant inhibitor dnXNOS1 and chemical inhibitors L-NAME or ETU) resulted in consistently similar phenotypes, attesting to the specificity of their action. In contrast to the action of the NOS inhibitors, elevating NO levels by injection of either XNOS1 mRNA (Fig. 2Bh) or NO donor SNAP (not shown) resulted in a smaller head, brain, and eye (46%,  $n = 55$  for XNOS1 and 51%,  $n = 90$  for SNAP); however, neither the course of gastrulation nor axis elongation were affected.

Together, the character of the defects induced by inhibition of NOS activity suggest that NO is involved in controlling several

extension (short, stunt embryos) and neural convergent extension (dorsal flexure and delayed closure of the neural tube).

To further link the action of the recombinant NOS inhibitor with a specific morphogenetic defect, we traced the site of expression of the injected dnXNOS1 mRNA by co-injecting it with GFP mRNA into the two dorsal blastomeres of the eight-cell embryo and analyzed the tadpole. This showed that the shortened axis phenotype was associated with the presence of the GFP tracer (and thus, dnXNOS1) in

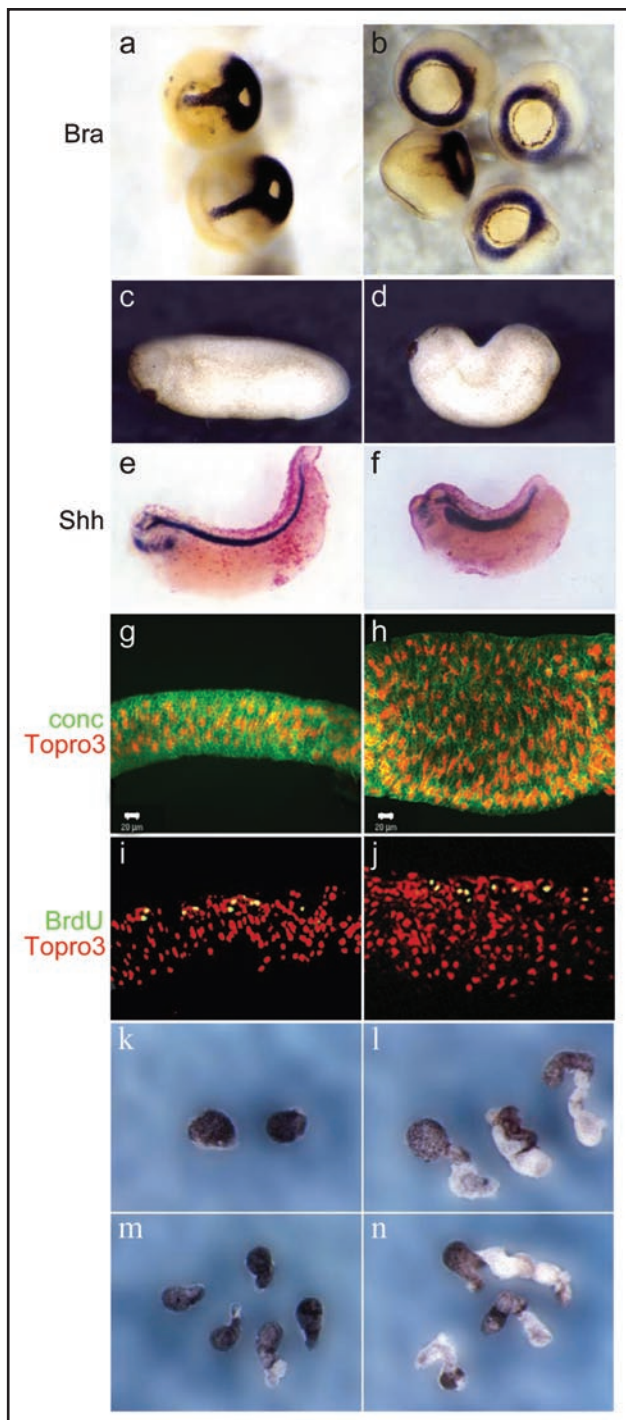


Figure 3. Inhibition of NOS distorts morphogenetic cell movements and axis elongation. (a and b) Inhibition of NOS does not affect mesodermal induction but distorts convergent extension. In situ hybridization with mesodermal marker Brachiury (Bra) of the late gastrula stage embryos which received injection of  $\beta$ -galactosidase mRNA (a) or dnXNOS1 mRNA (b). (c and d) Inhibition of NOS by dnXNOS1 results in shorter axis and dorsal flexure in tadpole stage embryos (d) as compared to the control embryos injected with  $\beta$ -galactosidase mRNA (c). (e and f) Inhibition of NOS by dnXNOS1 results in a thicker and shorter notochord (f) compared with the control (e). The notochord was revealed by in situ hybridization with a probe for Sonic hedgehog (Shh). (g and h) Notochords dissected from the stage 23 embryos injected dorsally at the four-cell stage with  $\beta$ -galactosidase (g) or dnXNOS1 (h) mRNA were stained with concanavalin A for membranes (green) and with Topro3 for nuclei (red). Note the defects in the cellular order and shape of the notochords after NOS inhibition. Bar is 20  $\mu$ m in (g–j). (i and j) BrdU labeling: the fraction of BrdU-labeled cells (yellow) does not change after injection of dnXNOS1 mRNA (j) as compared to the injection of  $\beta$ -galactosidase mRNA (i) (5+/-1% vs. 7+/-2%). (k–n) NOS inhibitor prevents, whereas NO donor allows, the elongation of the activin-treated animal caps isolated prior to gastrulation. (k) untreated control animal caps; (l) animal caps treated with activin; (m) animals caps treated with activin and L-NAME; (n) animal caps treated with activin and SNAP.

Brachiury (Bra) (Fig. 3a and b). However, at the late gastrula stage, in the embryos injected with dnXNOS1, the layout of posterior mesoderm, marked by the Bra expression, showed defects in cell movements as mesodermal cells failed to converge and extend the midline, leaving the blastopore wide open (Fig. 3b).

To further examine whether a deficit of NO impairs morphogenetic cell movements in the mesoderm during axis elongation we compared the notochords of embryos injected with dnXNOS1 mRNA or control  $\beta$ -galactosidase mRNA. dnXNOS1-injected embryos were shorter and showed distinct dorsal flexure (Fig. 3c and d) and, as axis continued to extend, the notochord (revealed by Shh staining) remained shorter and thicker (Fig. 3e and f). Analysis of dissected notochords revealed significant distortions of the normal cellular order in the notochords of the animals that received the NOS inhibitor (Fig. 3g and h), indicative of defects in mesodermal convergent extension. To examine whether inhibitor-induced changes in the mesoderm are due to the defects in cell movement or to the excessive number of cells that could, potentially, distort the movement, we analyzed cell proliferation in a BrdU-labeling experiment. The fraction of BrdU-labeled cells in the total cell number (mitotic index) in the notochords of dnXNOS1-injected embryos did not differ significantly from the control (5+/-1% vs. 7+/-2%, Fig. 3i and j) and was very low compared to the other embryonic tissues (consistent with studies showing cessation of cell division in the mesoderm after involution.<sup>29</sup> These results indicate that NO signaling is not necessary for suppression of cell division in the notochord during axis elongation. They also indicate that the observed changes in the notochord structure arise as a result of distorted mesodermal convergent extension rather than excessive cell division.

The importance of NO for cell movement was also evident in vitro, in embryonic explants (animal caps) induced by activin. Addition of activin induced elongation of 80% of the control explants (n = 41), (Fig. 3k and l). Adding NOS inhibitor L-NAME to the media prevented activin-induced elongation of 75% (n = 32) of the explants (Fig. 3m). In contrast, addition of the NO donor SNAP allowed animal caps to elongate in response to activin similarly to the control group (Fig. 3n). Together, the results of our in vivo

aspects of early *Xenopus* development: the enlargement of the tadpole organs suggests that NO may be involved in controlling cell division, the shortened anteroposterior axis indicates defects in the convergent extension of the mesoderm, whereas dorsal flexure and delayed closure of the neural tube suggest defects in neural convergent extension.

**NO in mesodermal convergent extension.** Orderly directional movement of the axial mesoderm during convergent extension and axis elongation is necessary for the formation of the rod-like structure of the notochord. Inhibition of NOS does not affect mesodermal induction, as judged by the expression of a mesodermal marker

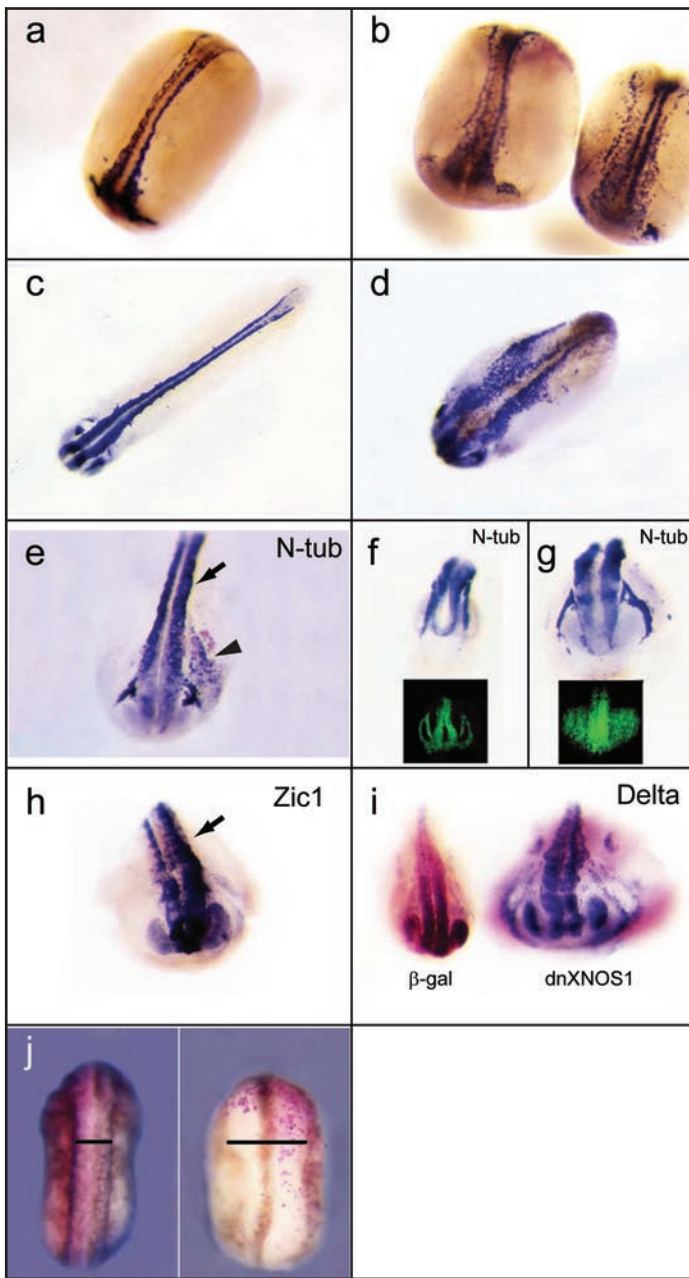


Figure 4. Inhibition of XNOS1 distorts neural convergent extension and induces excessive cell proliferation in the ectoderm. (a–d) In situ hybridization for N-tubulin at neurula (a, control embryo; b, embryo injected with NOS inhibitor) and tailbud (c, control embryo; d, embryo injected with NOS inhibitor) stages shows that inhibition of NOS results in a wider, shorter, and incompletely fused neural tube. (e–g) In situ hybridization at neurula stage with N-tubulin (e–g), Zic1 (h), and Delta (i) of embryos injected with dnXNOS1 mRNA and  $\beta$ -galactosidase (used as a tracer) mRNA (e, g, i) or with D-NAME (f) and L-NAME (g). In (e and h), embryos were injected into one blastomere of the two-cell embryo (arrow marks injected side, revealed by expression of  $\beta$ -galactosidase); note the widened neural tube (e and h) and ectopic N-tubulin-positive cells on the injected side of the embryo (e). In (i), embryos were injected into two dorsal blastomeres of the 4-cell embryo; note the enlarged anterior nervous system and a broader neural tube (control embryo on the left was injected with  $\beta$ -galactosidase mRNA only). In (f and g), embryos were injected at blastula stage with D-NAME (f) or L-NAME (g), labeled at stage 23 with BrdU, and analyzed for N-tubulin expression and BrdU incorporation (green, insets); note the wide neural tube and increased number of BrdU-labeled cells in embryos injected with L-NAME (g). (j) embryos injected with dnXNOS1 mRNA and raised in conditions blocking cell proliferation (media containing DNA synthesis inhibitors aphidicolin and hydroxyurea) (right) still display a wider neural tube than control embryos injected with  $\beta$ -galactosidase mRNA and grown under the same conditions (left), indicating that defects in cell movements caused by NOS inhibitors are independent of their effect on proliferation.

neural tube and enlarged the neural domain (marked by expression of N-tubulin) as seen both at neurula and tailbud stages (Fig. 4a–g). Enlarged neural tube was also detected using neuronal markers Zic1 and Delta (Fig. 4h and i) (note that in the experiments in Fig. 4e and 4h only one of the two blastomeres was injected with dnXNOS1). Furthermore, staining with N-tubulin revealed, in the injected side, numerous ectopic N-tubulin-positive cells away from the neural tube in the zone of the epidermis (Fig. 4e). In these experiments (as in the experiments of Fig. 2), chemical (Fig. 4b,d and g) or recombinant (Fig. 4e,h and i) inhibitors of NOS produced similar results, reconfirming the specificity of their action. Thus, expansion of the zone of cells expressing neuronal marker genes highlights the defects induced in the developing nervous system by the deficit of NO.

We further examined whether in the developing nervous system NO is involved in controlling cell proliferation (perhaps reflecting its ability to suppress cell division in several developmental contexts<sup>8–10,13,15,30</sup>). Incorporation of BrdU, tested at stage 23, was higher and occurred in a wider zone of the nervous system in embryos injected with inhibitor of NOS that in control embryos. (Fig. 4f and g). This suggests that the increased proliferation induced by NOS inhibition was likely to contribute to the enlarged neural tube (as revealed by N-tubulin expression). Importantly, however, when DNA synthesis was suppressed by aphidicolin and hydroxyurea<sup>31</sup> to deduct the contribution of increased cell proliferation to the observed phenotype (Fig. 4j), the neural tube remained wider and shorter in embryos injected with NOS inhibitors as compared to the controls. This shows that defects in neural convergent extension induced by inhibition of NOS activity are not merely consequences of increased cell proliferation and indicates an independent involvement of NO in cell movement.

Together, the observations of the wide and shorter neural tube and delayed fusion of the neural tube at neurula stage and of the dorsal flexure observed at tailbud stage indicate that NO is important for neural convergent extension. Furthermore, increased BrdU incorporation when NOS is inhibited indicates that NO is

and in vitro experiments suggest that in the axial mesoderm, NO does not affect cell division during axis elongation or mesodermal induction during gastrulation but is involved in regulating morphogenetic cell movements that underlie convergent extension and axis elongation.

**NO in neural convergent extension.** A wider neural tube, delay in neural tube closure, an open neural tube during neurulation, and dorsal flexure at the tailbud stage, seen in a large fraction of embryos injected with dnXNOS1, indicate that a deficit of NO affects neural convergent extension, whereas the enlarged organ size (including neural tissue, Fig. 2Bg) suggests excessive cell division. To further analyze the changes in morphogenesis induced by the suppressed production of NO, we probed the developing nervous system of the embryo at neurula and tailbud stages by in situ hybridization with neural marker N-tubulin. Suppression of NOS activity by injection of either recombinant or chemical NOS inhibitors shortened the

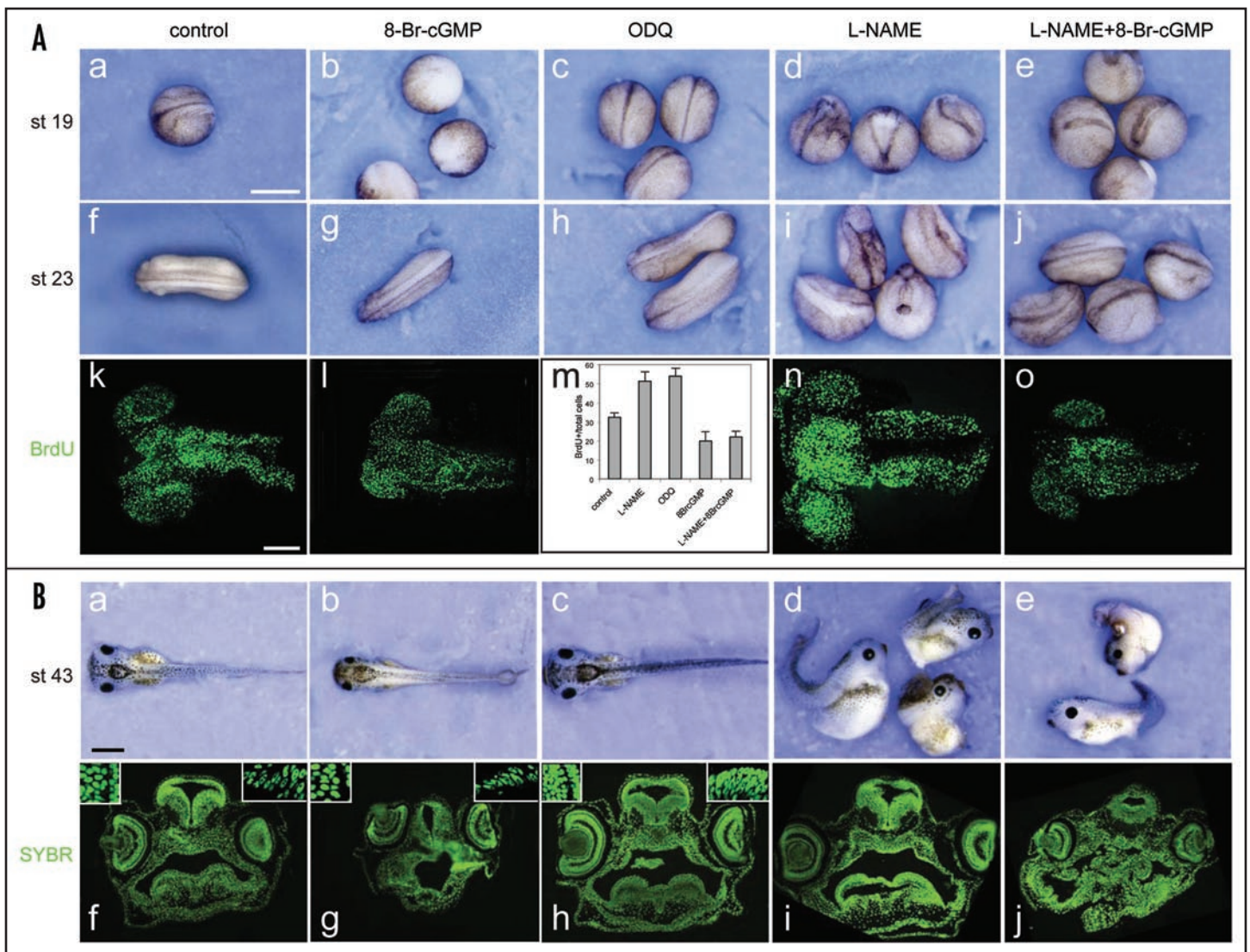


Figure 5. cGMP mediates the antiproliferative action of NO during early development. (A) Embryos were injected at blastula stage with saline, 8-Br-cGMP, ODQ, L-NAME, or L-NAME with 8-Br-cGMP; types of treatment are indicated. Part of the animals in each group were examined for phenotypic changes at stage 19 (a–e) and for the changes in phenotype and cell proliferation at stage 23 (f–o) (remaining animals were analyzed at stage 43, see Fig. 5B). For the analysis of cell proliferation in the developing neural tube, embryos were labeled with BrdU at stage 23 for 2 hr and neural tubes were dissected and analyzed for cell proliferation by staining for BrdU-positive cells (green) (k–o) and for the total number of cells by staining with Topro3. (m) shows mitotic indices in the neural tube for each treatment calculated as a ratio of BrdU-positive to the total (Topro3-stained) cells: BrdU incorporation is increased in the neural tube of animals treated with L-NAME and ODQ and decreased in animals treated with 8-Br-cGMP or with 8-Br-cGMP in combination with L-NAME. For both (A and B), bar is 1 mm for the images of whole embryos and 200  $\mu$ m for the images of BrdU-labeling experiments. (B) Embryos from the same experimental groups as in (A) were examined at stage 43; types of treatments correspond to those in (A). The animals were analyzed for morphology (a–e) and then examined by sectioning and staining the nuclei with SYBR Green (f–j). In 5Bf–j, insets on the left of the image show high magnification view of the retina of the eye, insets on the right show high magnification view of the tectum area of the brain; note the reduced cell number in the retina and the brain of the 8-Br-cGMP-treated embryos and the increased cell number and cell density in these areas in the ODQ-treated animals.

also important for restricting cell division in the developing nervous system during axis elongation. This dual action of NO in the neuroectoderm contrasts with its action in the axial mesoderm where it is important for the regulation of convergent extension but not cell division.

**cGMP-dependent pathway controls antiproliferative action of NO.** We next examined whether soluble guanylate cyclase (sGC), a major effector of the action of NO, is involved in NO-mediated control of cell movement and cell proliferation during embryonic development in *Xenopus*. We used 8-Bromo-cyclic guanylate monophosphate (8-Br-cGMP) and sGC inhibitor 1H-[1,2,4]-oxadiazolo-[4,3- $\alpha$ ]-quinoxalin-1-one (ODQ), to activate or suppress

cGMP signaling, respectively. When 8-Br-cGMP was injected at the blastula stage, the embryos, while maintaining apparently normal body shape, entered neurulation with a slight delay and appeared smaller during axis elongation (stage 23; Fig. 5Aa,b,f and g). BrdU labeling of stage 23 embryos indicated that an increase of cGMP levels inhibits cell proliferation. (Fig. 5Ak and l). In contrast, sGC inhibitor ODQ increased cell proliferation in neural tube, acting similarly to NOS inhibitor L-NAME (Fig. 5Am and n). However, unlike L-NAME, ODQ did not induce defects in axis elongation and morphogenesis (Fig. 5Ac and h). These experiments suggest that

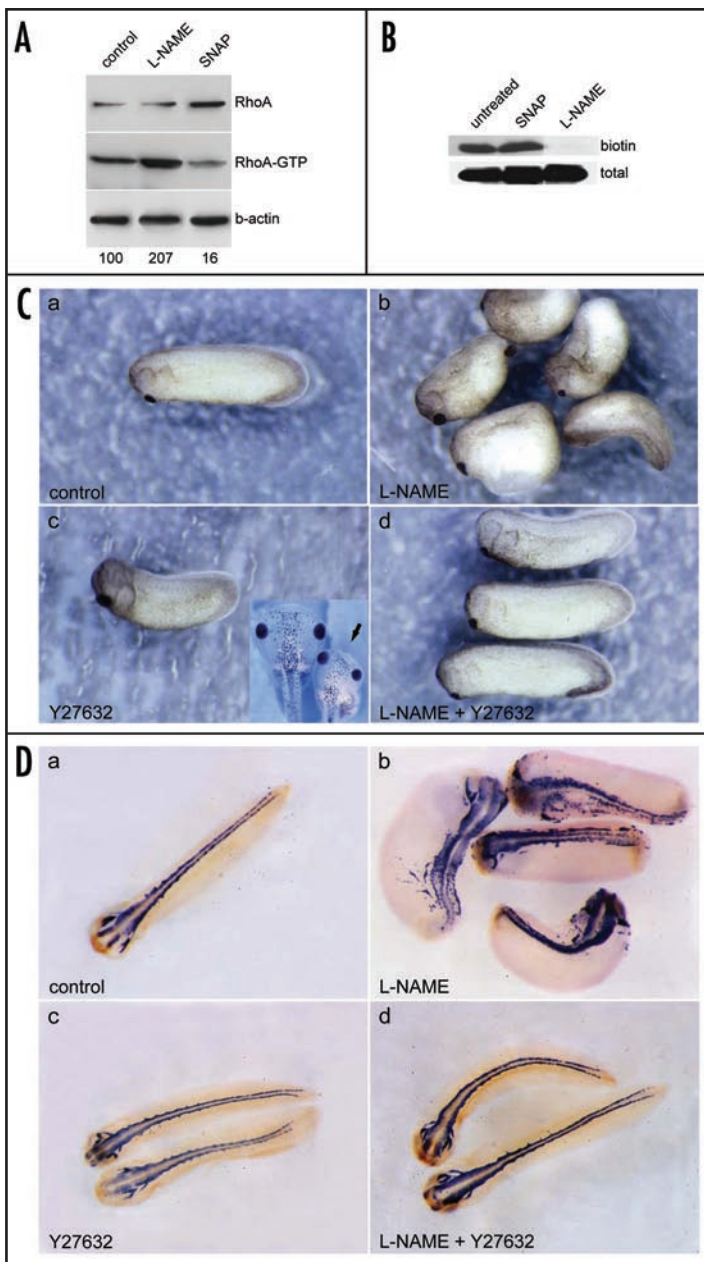


Figure 6. NO regulates early development through suppression of RhoA-ROCK. (A) NO negatively controls RhoA activity. Embryos were injected with either NO donor SNAP, NOS inhibitor L-NAME, or saline, and protein extracts were examined for RhoA activity. Active (GTP-bound) RhoA molecules were pulled down after incubation with Rhotekin-beads and analyzed by Western blotting with anti-RhoA antibody. Upper bands show the total expression of RhoA in the extracts. The numbers below each lane represents the fraction of the active RhoA molecules within the total RhoA molecules, with the levels in untreated embryos taken as 100%. (B) S-nitrosylation of RhoA. S-nitrosylation status was examined using the biotin switch assay after transfection of RhoA-T7 constructs into bend.3 cells and probed using antibody to the T7 tag. (C and D) Inhibition of ROCK rescues the defects induced by inhibition of NOS. (C) Embryos were injected at blastula stage with saline (a), L-NAME (b), ROCK inhibitor Y27632 (c; inset shows microcephaly of the Y27632-injected embryos at the tadpole stage, injected embryo is marked by arrow, control embryo on the left), or L-NAME with Y27632 (d). (D) In situ hybridization for N-tubulin of the same experimental groups of animals. Embryos injected with L-NAME (Cb and Db) show defects in axis elongation and neural tube formation; also note a more intense N-tubulin staining, larger anterior nervous system and numerous scattered neurons off the neural tube. Injection with Y27632 along with L-NAME rescued the defects of the L-NAME-injected embryos and normalized axis extension and neural tube formation (Cd and Dd).

importantly, however, unlike the changes induced by NOS inhibitors, the action of ODQ was not accompanied by defects in convergent extension or axis elongation at the tadpole stage. As seen at earlier stages, embryos co-injected with 8-Br-cGMP and L-NAME were smaller than control embryos or L-NAME-injected embryos but still showed defects in convergent extension; i.e., 8-Br-cGMP prevented the increase in cell number induced by the NOS inhibitor (and even reduced it compared to the control) but did not rescue the defects in convergent extension and axis elongation induced by the inhibitor (Fig. 5Bd,e,i and j).

Together, these results indicate that NO acts on cGMP-dependent pathways to suppress cells proliferation in the developing nervous system. They also indicate that NO uses cGMP-independent pathways to exert its effects on morphogenetic cell movements. Furthermore, these data provide additional support to our conclusion that the effects of NO on cell motility are independent of those on cell division and demonstrate that these effects can be uncoupled through modulation of cGMP production.

**NO acts as a negative regulator of RhoA-ROCK signaling.** When analyzing the pattern of XNOS1 expression in the dorsal mesoderm during gastrulation and neurulation (Fig. 1Ac and h), we noticed that it resembled that of RhoA,<sup>32</sup> whose activity is critical for morphogenetic cell movement in *Xenopus*.<sup>32-34</sup> The effect of RhoA on cell migration and cell proliferation is regulated by NO in several contexts;<sup>17,35-38</sup> furthermore, phosphorylation of RhoA by cGMP-dependent protein kinase (PKG) inhibits RhoA activity.<sup>39</sup> Based on these observations, we asked whether RhoA may mediate the action of NO during *Xenopus* development.

To investigate whether NO controls RhoA activity, we analyzed the active GTP-bound form of RhoA in early tailbud stage embryos injected, prior to gastrulation, either with the NO donor SNAP or the NOS inhibitor L-NAME (Fig. 6A). Exposure to the NO donor decreased the amount of the GTP-bound form of RhoA as a fraction of total RhoA. In contrast, NOS inhibitor resulted in an increase in the fraction of the active form. This indicates that NO acts as a negative regulator of RhoA activity during the early stages of *Xenopus* development.

cGMP-dependent signaling may underlie the effect of NO on cell proliferation, but not on cell movement. Indeed, when we examined whether 8-Br-cGMP can rescue the defects induced by NOS inhibitor, we found that, although the L-NAME-induced increase in cell proliferation in the neural tube was suppressed by 8-Br-cGMP (Fig. 5An and o), the defects in cell movements seen as a thicker neural tube and a shorter axis, were still apparent (Fig. 5Ad,e,i and j).

We next examined the animals at the tadpole stage 43. Among 8-Br-cGMP injected animals, 90% (n = 72) looked smaller overall (Fig. 5Ba and b) and, after sectioning, showed reduced cell number in the brain and the eye (nuclear staining of the sections with SYBR-Green; Fig. 5Bf and g). In contrast, injection of ODQ resulted in an increased size of the embryo and increased cell number and cell density in the brain and the eye (72%, n = 85; Fig. 5Bc and h). This effect of ODQ resembles the action of NOS inhibitors;

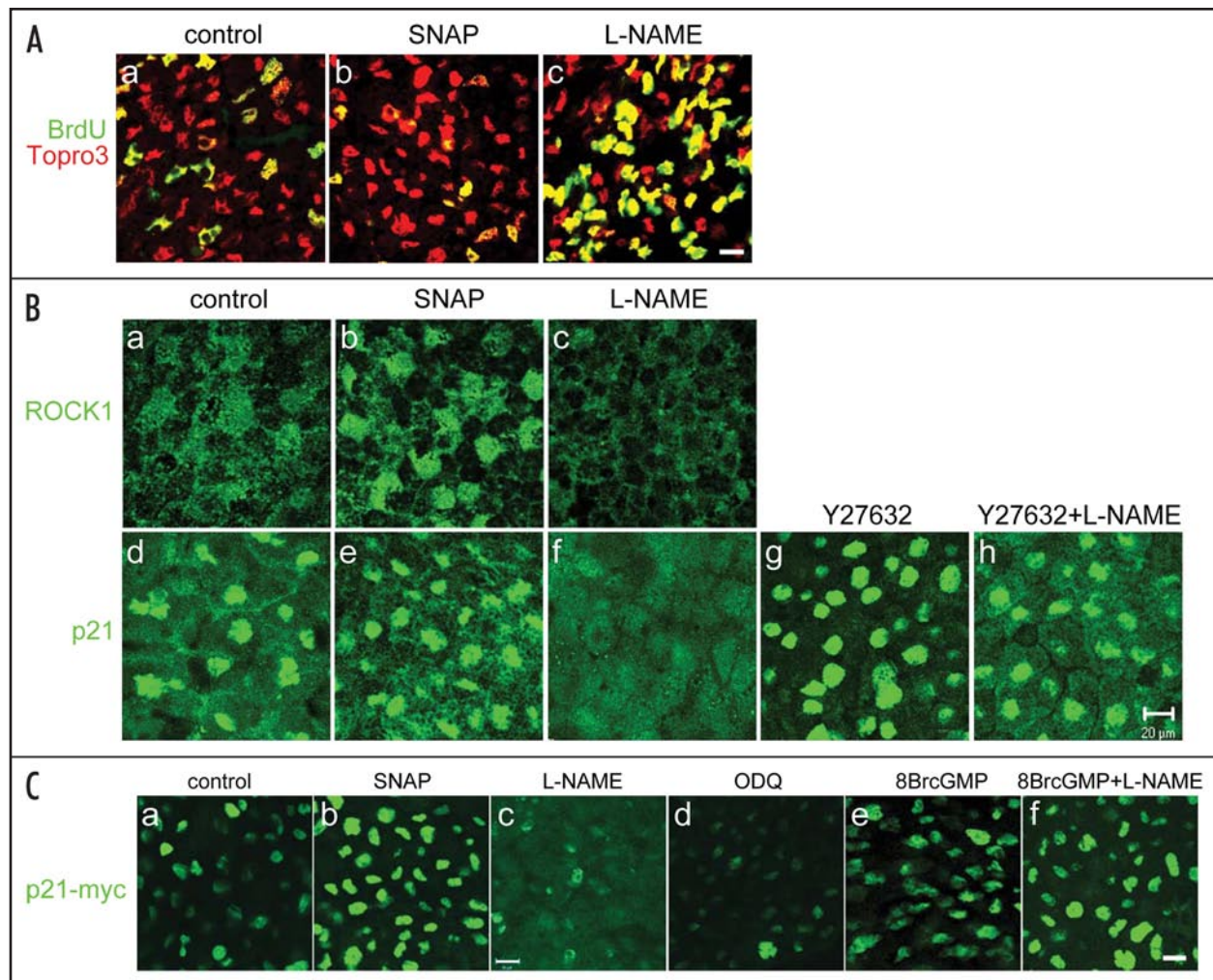


Figure 7. NO controls cell proliferation and cellular distribution of ROCK and p21WAF1 in animal caps. (A) NO regulates cells proliferation in the animal caps. NO donor SNAP suppresses cell proliferation in the ectoderm of animal caps (b), whereas NOS inhibitor L-NAME induces excessive cell proliferation (c), as compared to the control (a). Red - Topro3 staining of nuclei, green - BrdU labeling of dividing cells. Bar is 20  $\mu$ m in a-c. (B) NO controls the cellular distribution of ROCK and p21WAF1. (a-c) animal caps stained with anti-ROCK1 antibody; types of treatments are indicated. Note an increase in the number of cells with nuclear localization of ROCK1 after incubation with SNAP (b), and a decrease after incubation with L-NAME (c). Experiments with antibodies to ROCKII gave similar results (not shown). (d-h) animal caps stained with anti-p21WAF1 antibody; types of treatment are indicated. p21WAF1 localizes primarily in the nuclei in untreated cells (d); exposure to SNAP increases (e), whereas exposure to L-NAME strongly decreases (f), the fraction of cells with nuclear localization of p21WAF1. Addition of Y27632 to L-NAME (h) reverses the changes induced by L-NAME and restores a predominantly nuclear localization of p21WAF1. Bar is 20  $\mu$ m in (a-h). (C) sGC mediates the effect of NO on the cellular distribution of p21WAF1. Fertilized eggs were injected with trace amounts of mRNA coding for p21WAF1-myc protein fusion and animal caps derived from the embryos were treated with L-NAME, SNAP, ODQ, 8-Br-cGMP, and L-NAME with 8-Br-cGMP (types of treatment are indicated); distribution of p21WAF1-myc was followed by staining with anti-myc antibody. The changes in the cellular distribution of the myc-tagged p21WAF1-myc in response to L-NAME and SNAP are similar to those of the endogenous p21WAF1 (compare to Fig. 7Bd-h). ODQ, an inhibitor of sGC activity, decreases nuclear accumulation of p21WAF1-myc. Treatment with 8-Br-cGMP stimulates nuclear accumulation of p21WAF1-myc and is able to overcome the action of the NOS inhibitor L-NAME and retain p21WAF1-myc in the nucleus. Bar is 20  $\mu$ m in (a-f).

An important mechanism of protein regulation by NO is via S-nitrosylation of cysteine residues.<sup>40</sup> We probed the nitrosylation status of RhoA in NO-producing cells by employing the biotin-switch method<sup>25</sup> and found nitrosylated RhoA molecules in the cell extracts (Fig. 6B). This modification could not be detected when cells were incubated with NOS inhibitor L-NAME, confirming that RhoA is nitrosylated by the action of NOS *in vivo*.

Since excessive activity of RhoA may underlie the phenotypes resulting from inhibition of NOS activity and since in many settings RhoA action is mediated by RhoA-dependent kinase ROCK, we asked if inhibition of ROCK can compensate for increased RhoA

signaling and rescue the defects induced by inhibition of NOS. We found that injection of Y27632, a specific inhibitor of ROCK, in conjunction with dnXNOS1 or L-NAME rescued the defects caused by NOS inhibitors and restored the normal phenotype in 70% (n = 40) of the affected embryos (analyzed at the tailbud stage, Fig. 6C and D): it restored normal axis extension and neural tube folding, eliminated dorsal flexure, prevented the appearance of ectopic neurons away from the neural tube, and normalized anterior neural tube formation. Y27632 alone did not elicit noticeable changes in the developing embryo and the nervous system of the tailbud-stage embryo (except for the embryos appearing slightly smaller overall);

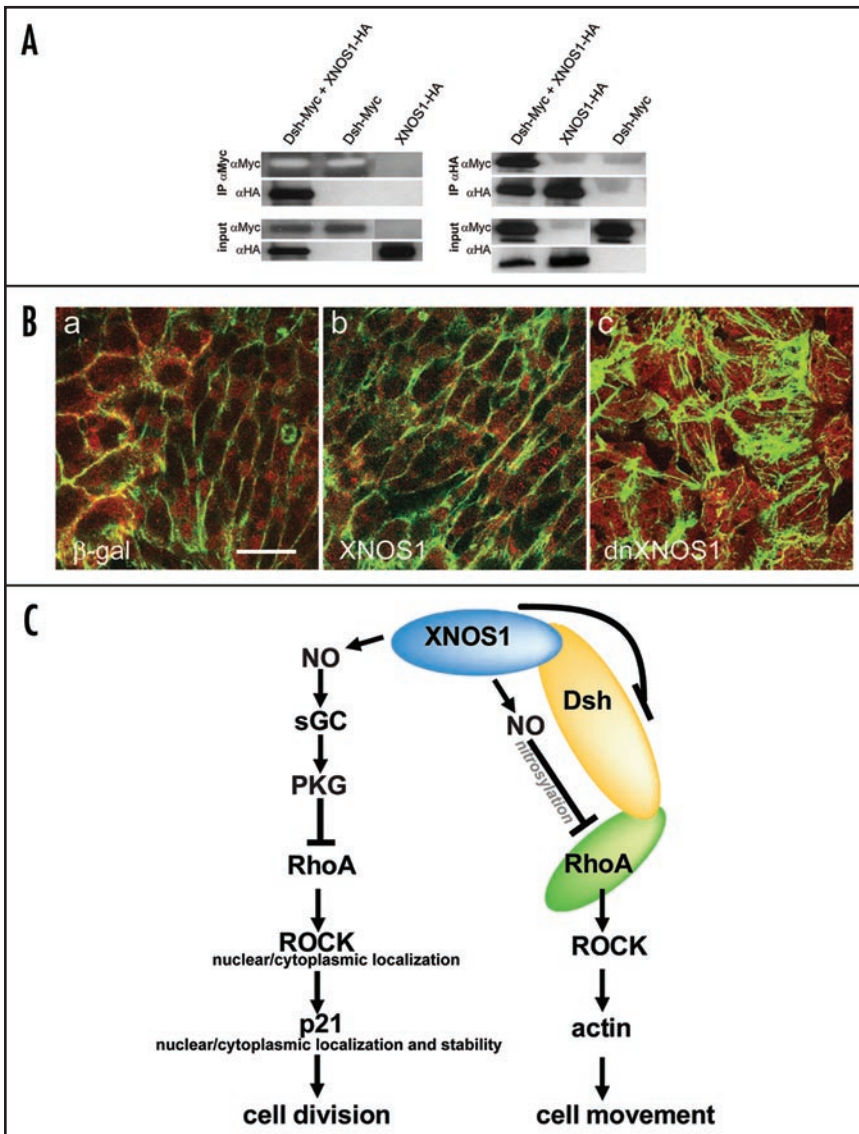


Figure 8. (A) Dsh interacts with XNOS1. Cultured HEK293 cells were transfected with recombinant constructs coding for XNO-HA and Dsh-myc protein fusions separately or together. Protein complexes were immunoprecipitated from the cell lysates using antibodies to the HA and myc epitopes and the same antibodies were then used to probe the presence of Dsh and XNOS1 in the complexes using Western blots; antibodies used for immunoprecipitation and for Westerns are indicated. Input refers to the starting material. Due to large differences in the signal strength, for some of the lanes images of different exposures are combined. Amount of Dsh-myc protein in two top left lanes is very high and the band signals are oversaturated. (B) XNOS1 regulates the distribution of Dsh and the organization of the actin cytoskeleton. 2 dorsal blastomeres of the 4-cell embryo were injected with XNOS1, dnXNOS1, or  $\beta$ -galactosidase mRNA and neural tube was dissected from the epidermis at stage 28, stained in whole mount with anti-Dsh antibody (red) and falloidin (for polymerized actin) (green), flattened on the slide and the images oriented on the figures by lateral side down and medial side up. Note the loss of the spindle-like shape, the increased levels and loss of polarized distribution of Dsh, and the loss of the preferential localization of the actin filaments in cells of the embryos injected with dnXNOS1 mRNA but not with XNOS1 mRNA. Bar is 20  $\mu$ m. (C) Schematic representation of two signaling pathways mediating the action of XNOS1 on cell division and cell movement during early *Xenopus* development.

later, at the tadpole stage, 81% ( $n = 70$ ) of the Y27632-injected embryos developed microcephaly (Fig. 6Cc, inset). Together, our data indicate that the RhoA-ROCK pathway mediates the action of NO upon both cell proliferation and cell movement during early development of *Xenopus*.

To gain insight into how the RhoA-ROCK pathway may link NO to cell cycle regulation, we examined how modulation of NO levels affects cell proliferation and localization of ROCK in animal caps (consisting, in the absence of activin, of ectodermal cells). BrdU labeling of animal caps isolated at blastula stage and cultivated until their intact sibling reached neurula stage showed that NO donor SNAP resulted in a decrease in cell proliferation, while NOS inhibitor L-NAME resulted in excessive proliferation (Fig. 7Aa–c), an observation consistent with the data obtained on several animal models.<sup>8–10,12,14</sup>

In control animal caps ROCK localization was mainly cytoplasmic but ROCK was also detected in the nucleus of a fraction of the cells (Fig. 7Ba). The NO donor SNAP increased the number of cells with nuclear localization of ROCK (Fig. 7Bb). In contrast, the NOS inhibitor L-NAME drastically decreased the number of cells with nuclear localization of ROCK (Fig. 7Bc). Thus, our data indicate that in ectodermal cells NO regulates the distribution of ROCK between the nucleus and cytoplasm.

In cultured cells, ROCK can be detected in a complex with the cyclin-dependent kinase (cdk) inhibitor p21WAF1 and cytoplasmic sequestration of this complex prevents cell cycle arrest.<sup>41,42</sup> We asked whether NO, by controlling the distribution of ROCK, may also affect the distribution of p21WAF1 in animal cap cells. We found that the levels of p21WAF1 in the nucleus change, in a manner similar to ROCK, in response to changes in the level of NO: NO donors caused accumulation of p21WAF1 in the nucleus (thus permitting it to induce cell cycle arrest), whereas NOS inhibitors resulted in a decrease in the levels of p21WAF1 and its depletion from the nucleus (thus segregating p21WAF1 from the cdk's and preventing cell cycle arrest) (Fig. 7Bd–f). Importantly, treatment of the animal caps with Y27632 together with NOS inhibitors reversed the effect of the NOS inhibitors and restored the presence of p21WAF1 in the nucleus thus reversing the effect of the NOS inhibitors (Fig. 7Bg and h). This suggests that in the ectoderm NO controls cell proliferation by regulating the distribution of p21WAF1 between the nucleus and the cytoplasm via the RhoA-ROCK pathway.

To further confirm that the distribution of p21WAF1 is regulated by NO and to investigate the signals involved, we injected fertilized eggs with trace amounts of mRNA coding for p21WAF1 tagged with the c-myc epitope and followed the localization of p21WAF1-myc in animal caps treated with SNAP, L-NAME, ODQ, or 8-Br-cGMP. We found that recombinant p21WAF1-myc responded to the NO donor and inhibitor in a manner similar to the endogenous p21WAF1 protein: it accumulated in the nucleus in response to SNAP but was mostly absent from the nucleus in response to L-NAME (Fig. 7Ca–c). Moreover, its pres-

ence in the nucleus was decreased in most of the cells of animal caps treated with ODC and, conversely, was increased in the nucleus in cells treated with 8-Br-cGMP (Fig. 7Cd and e). Importantly, it was still in the nucleus when cells were treated with a combination of 8-Br-cGMP and L-NAME (Fig. 7Cf). Together, these observations confirm that NO regulates the accumulation of p21WAF1 in the nucleus; suggest that the NO-induced effects are independent of p21WAF1 transcriptional activity (note that the myc-tagged p21WAF1 protein encoded by the injected mRNA parallels the behavior of the endogenous p21WAF1); indicate that this distribution is mediated by the sGC-cGMP signaling; and suggest that, in its effects on p21WAF1, cGMP signaling is downstream of the NO-production step (since the effect of 8-Br-cGMP trumps the effect of NOS inhibitor L-NAME).

**PCP pathway mediates the action of NO on cell movement.** Taken together, our results suggest that the action of NO on cell division in the developing embryo depends on the cGMP signaling pathway. In contrast, the effect of NO on cell movement is not dependent on cGMP, suggesting that it is mediated by other signaling pathways. We therefore examined possible interactions between NO and the Wnt-Frizzled-Dsh pathway, a major pathway in the developing *Xenopus* embryo that controls PCP required for directional cell movements. Dsh is a critical component of this pathway, serving as a scaffold and organizing protein complexes which regulate cytoskeletal remodeling, cell polarization, and cell movement. Accumulation of Dsh at the cell membrane is essential for convergent extension (removal of Dsh from the cell membranes disrupts convergent extension;<sup>43</sup> furthermore, the overall level of Dsh is also critical since suppression of Dsh degradation can also disrupt convergent extension<sup>44</sup>).

We first examined interactions between XNOS1 and Dsh and the effects of NO on the cellular distribution of Dsh. When cultured cells were transfected with HA-tagged XNOS1 and myc-tagged Dsh, and protein interactions were probed by immunoprecipitation and Western blot analysis, we found that XNOS1-HA was present in protein complexes immunoprecipitated with an antibody to the myc epitope (and thus to Dsh-myc) and, conversely, Dsh-myc was present among proteins immunoprecipitated with an antibody to HA epitope (and thus, to XNOS1-HA) (Fig. 8A). This demonstrates that XNOS1 is present in protein complexes with Dsh and suggests that these proteins may interact *in vivo* (XNOS1 and Dsh have PDZ domains that may render them capable of such interaction).

We next examined the distribution of endogenous Dsh in embryos injected with either XNOS1 or dnXNOS1; we also analyzed the status of the actin cytoskeleton. We found that in the cells of the posterior part of the neural tube undergoing convergent extension, Dsh was localized near the membranes and accumulated near the tips of the spindle-shape cells (Fig. 8Ba). In these cells actin filaments were confined to the cell periphery. Overexpression of XNOS1 did not distort the spindle-like shape of the cells, the organization of the actin cytoskeleton, or the polarized distribution of Dsh (Fig. 8Bb). In contrast, in embryos injected with dnXNOS1 mRNA, cells lost their spindle-like shape, the actin filaments lost their preferential peripheral localization and instead formed extensive network across the cell, whereas Dsh became more abundant, lost its polarized distribution and was present throughout the cell (Fig. 8Bc).

Together these experiments suggest an interaction between XNOS1 and Dsh, regulation of Dsh distribution and levels by XNOS1, and the role of XNOS1 in controlling cell shape and planar

polarity. Deficit of NO distorts the planar polarity of the Dsh distribution in cells engaged in convergent extension and elevates its levels, disrupts the spindle-like cell shape that is essential for their directed movement during convergent extension, and alters the organization of the actin cytoskeleton by creating extensive intracellular filament networks; these changes may underlie the observed defects in cell movement during convergent extension.

## DISCUSSION

We have identified NO as a signal that coordinates morphogenetic movements with the cell cycle during the development of *Xenopus* embryo. NO both suppresses cell division and facilitates cell movement. This dual action of NO is crucial in the developing neural tissue where cells divide while undergoing convergent extension; in the axial mesoderm, where cell division largely ceases before the process of convergent extension, NO acts to facilitate cell movement without affecting cell proliferation.

Our results suggest a model where XNOS1 acts through two separate signaling pathways to control cell division and cell movement (Fig. 8C). XNOS1 regulates cell division via a cGMP-dependent pathway: XNOS1-produced NO activates sGC which, through production of cGMP, activates PKG. PKG is known to negatively regulate RhoA<sup>39</sup> and we consider that it is acting similarly in this pathway; thus, production of NO inhibits RhoA activity and the signaling from RhoA to ROCK. This leads to the observed nuclear accumulation of ROCK and p21WAF1, permitting inhibitory interactions of p21WAF1 with cdks and subsequent cell cycle arrest. Inhibition of XNOS1 activity diminishes production of cGMP, increases RhoA and ROCK activity, and prevents nuclear accumulation of p21WAF1, thus segregating it from its nuclear targets and interfering with its ability to halt the cell cycle, eventually leading to an increase in cell number; inhibition of ROCK restores the nuclear accumulation of p21WAF1 and rescues the NOS inhibitors-induced changes in cell proliferation. Inhibition of NOS only affects cell division in the neuroectoderm; thus, this pathway defines the antiproliferative action of NO in neural tissue.

In this model, XNOS1 regulates cell movement via a cGMP-independent pathway, where it interacts with Dsh, a central component of the PCP pathway. XNOS1 complexes with Dsh (perhaps through the PDZ domains of each protein) and controls planar polarity and turnover of Dsh. Dsh acts as a positive regulator of RhoA and they are found together in a complex; thus, Dsh may serve to mediate the interaction between XNOS1 and RhoA (perhaps involving Daam1<sup>33</sup>) and allow S-nitrosylation of RhoA by NO, leading to further suppression of RhoA activity.<sup>38</sup> Hence, apart from activating cGMP signaling, XNOS1 may exert its negative effect on RhoA through two additional mechanisms: through the control of the distribution and overall levels of Dsh and through nitrosylation of RhoA. RhoA regulates ROCK and, eventually, the remodeling of the actin cytoskeleton necessary for convergent extension. Inhibition of XNOS1 compromises appropriate cellular distribution and degradation of Dsh, increases RhoA activity, augments RhoA-ROCK signaling, hinders actin remodeling by ROCK, establishes a dense actin network throughout the cell, changes the cell shape, and leads to defects in convergent extension; inhibition of ROCK counteracts the action of NOS inhibitors and rescues the defects in convergent extension. Inhibition of NOS affects cell movement both in the

neuroectoderm and in the axial mesoderm; thus, this pathway defines the action of NO during both neural and mesodermal convergent extension.

Thus, our model implies that during development, cell division and cell motility, two critical processes which underlie tissue growth and morphogenetic movements (such as convergent extension), rely on the same signaling molecule, NO. Thus changes in NO availability affect both cell division and cell movements in a reciprocally coordinated manner: an increase in NO production suppresses cell proliferation and facilitates cell movement; conversely, a decrease in NO production increases cell proliferation and impairs cell movement. Since NO is a diffusible messenger and can function in both autocrine and paracrine modes, it may coordinate division and motility between adjacent cells and thus, both within and between different cell layers and tissues.

This model reflects our conclusion that cell division and cell movement are controlled through different mechanisms and can be experimentally uncoupled. This conclusion is supported by several observations: proliferation can be increased by ODQ without apparent defects in morphogenetic movements (Fig. 5Ac,h,m and Bc,h); excessive proliferation, but not distorted cell movement, induced by NOS inhibitors can be rescued by 8-Br-cGMP (Fig. 5Ae,j,o and Be,j); when proliferation is suppressed by aphidicolin and hydroxyurea, convergent extension defects induced by NOS inhibitors are still apparent (Fig. 4j); inhibition of NOS induces defects in convergent extension of non-dividing cells in the notochord (Fig. 3g–j). Thus, suppression or augmentation of cell division through the cGMP pathway does not have a direct effect on morphogenetic movements; conversely, defects in convergent extension, induced by the inhibition of NOS, cannot be rescued by suppressing cell division.

Interestingly, our observations suggest that cell proliferation and cell movement may be controlled by different levels of NO: changes in cell proliferation (BrdU incorporation and the size of the neural tube) were evident at lower concentration of NOS inhibitors than changes in cell movement (dorsal flexure and stunted body). This suggests that low levels of NO may induce cell motility, whereas cell cycle arrest may require higher concentrations of NO. These two different thresholds for the effects of NO provide additional support for our two pathways model.

Our results highlight RhoA as a crucial target of NO during development. NO acts as a negative regulator of RhoA activity and this may be achieved through at least three distinct mechanisms: activation of the sGC and cGMP signaling, control of accumulation and cellular distribution of Dsh, and S-nitrosylation of RhoA. The cGMP branch may act through activation of PKG and inhibitory phosphorylation of RhoA signaling (e.g., by augmenting the binding of RhoA to guanine dissociation factor (GDI)).<sup>39</sup> The importance of controlling Dsh is related to the fact that the planar polarity of Dsh distribution is necessary for convergent extension<sup>2</sup> and that Dsh localization to the cell membrane is crucial to its ability to activate RhoA during convergent extension;<sup>43</sup> furthermore, control of the intracellular levels of Dsh is critical for its proper action during convergent extension.<sup>44</sup> Finally, our finding that RhoA is S-nitrosylated by NO *in vivo* and that inhibition of NOS increases its activity raises a possibility that nitrosylation of critical cysteine residue(s) in RhoA may inhibit its activity, either directly, or by

affecting its interactions with regulatory proteins (e.g., GEFs, GAPs or GDIs); indeed, a recent report demonstrates that S-nitrosylation of RhoA inhibits its activity.<sup>38</sup>

Our finding that the ROCK inhibitor Y27632 rescues both excessive cell proliferation and impaired axis extension caused by a deficit of NO supports the notion that signaling from XNOS1 to RhoA-ROCK is crucial for both cell division and morphogenetic cell movements. However, the results with cGMP pathway agonists and antagonists indicate that the proliferation- and movement-related control of the RhoA-ROCK module by NO is achieved through different mechanisms and can be uncoupled. Furthermore, our conclusion that RhoA is involved in both pathways that mediate NO action during early *Xenopus* development is consistent with the reported effects of loss- and gain-of-function mutations of RhoA in the *Xenopus* embryo: several of the changes (reduced eyes, smaller neural tubes, and microcephalic phenotypes) seen when RhoA activity is inhibited<sup>32</sup> are phenocopied by the changes induced by overexpression of XNOS1, a negative regulator of RhoA, whereas inhibition of directional cell movement and convergent extension induced by the constitutively active form of RhoA<sup>32–34</sup> is phenocopied by inhibition of XNOS1.

NO and RhoA pathways interact in several physiological settings, with NO acting as a negative regulator of RhoA-mediated signaling (smooth muscle cell motility,<sup>17</sup> vasodilation in the aorta,<sup>35</sup> insulin-induced vasorelaxation,<sup>37</sup> and erectile response<sup>36</sup>). We now show that cross-talk between the NO and RhoA pathways is more widespread and is critical for early *Xenopus* development. More generally, the molecular mechanism we outline may be extensively employed in various contexts to transduce NO signals during cell differentiation and organism development.

We have discovered that NO regulates and coordinates cell division and cell movement in early vertebrate development. Deficits in NO availability, by uncoupling these tightly coordinated processes, may underlie developmental abnormalities, for instance, neural tube defects in human development. It is possible that the system of reciprocal NO control of cell proliferation and cell movement has been evolved because under certain circumstances division and motility may be fundamentally temporally incompatible and NO is employed to permit one process to occur while simultaneously holding the other in check.

#### Acknowledgements

We are grateful to David Helfman, Paul Krieg, Shin-Ichi Ohnuma, Yoshiki Sasai, Sergei Sokol, and Linda van Aelst for the recombinant constructs and reagents. We thank Stephen Hearn for his excellent assistance with confocal microscopy and to Barbara Mish for help with experiments. We are grateful to David Helfman, Linda van Aelst, and Julian Banerji for fruitful discussion, to Julian Banerji for the critical reading of the manuscript, and to the organizers of the CSHL *Xenopus* early development course, Paul Krieg and Sally Moody for invaluable advice. This work supported by the NIH, the NSF, the Cody Center for Autism and Developmental Disabilities, the Seraph Foundation, the Henry Charles Leach Foundation, and the Ira Hazan Fund.

## References

1. Keller R, Davidson LA, Shook DR. How we are shaped: The biomechanics of gastrulation. *Differentiation* 2003; 71:171-205.
2. Wallingford JB, Fraser SE, Harland RM. Convergent extension: The molecular control of polarized cell movement during embryonic development. *Dev Cell* 2002; 2:695-706.
3. Ohnuma S, Harris WA. Neurogenesis and the cell cycle. *Neuron* 2003; 40:199-208.
4. Klein TJ, Mlodzik M. Planar cell polarization: An emerging model points in the right direction. *Annu Rev Cell Dev Biol* 2005; 21:155-76.
5. Leptin M. Gastrulation movements: The logic and the nuts and bolts. *Dev Cell* 2005; 8:305-20.
6. Seifert JR, Mlodzik M. Frizzled/PCP signalling: A conserved mechanism regulating cell polarity and directed motility. *Nat Rev Genet* 2007; 8:126-38.
7. Ciruna B, Jenny A, Lee D, Mlodzik M, Schier AF. Planar cell polarity signalling couples cell division and morphogenesis during neurulation. *Nature* 2006; 439:220-4.
8. Enikolopov G, Banerji J, Kuzin B. Nitric oxide and *Drosophila* development. *Cell Death Differ* 1999; 6:956-63.
9. Gibbs SM. Regulation of neuronal proliferation and differentiation by nitric oxide. *Mol Neurobiol* 2003; 27:107-20.
10. Contestabile A, Ciani E. Role of nitric oxide in the regulation of neuronal proliferation, survival and differentiation. *Neurochem Int* 2004; 45:903-14.
11. Villalobo A. Nitric oxide and cell proliferation. *Febs J* 2006; 273:2329-44.
12. Peunova N, Scheinker V, Cline H, Enikolopov G. Nitric oxide is an essential negative regulator of cell proliferation in *Xenopus* brain. *J Neurosci* 2001; 21:8809-18.
13. Moreno-Lopez B, Romero-Grimaldi C, Noval JA, Murillo-Carretero M, Matarredona ER, Estrada C. Nitric oxide is a physiological inhibitor of neurogenesis in the adult mouse subventricular zone and olfactory bulb. *J Neurosci* 2004; 24:85-95.
14. Packer MA, Hemish J, Mignone JL, John S, Pugach I, Enikolopov G. Transgenic mice overexpressing nNOS in the adult nervous system. *Cell Mol Biol (Noisy-le-grand)* 2005; 51:269-77.
15. Packer MA, Stasiv Y, Benraiss A, Chmielnicki E, Grinberg A, Westphal H, Goldman SA, Enikolopov G. Nitric oxide negatively regulates mammalian adult neurogenesis. *Proc Natl Acad Sci USA* 2003; 100:9566-71.
16. Noiri E, Peresleni T, Srivastava N, Weber P, Bahou WF, Peunova N, Goligorsky MS. Nitric oxide is necessary for a switch from stationary to locomoting phenotype in epithelial cells. *Am J Physiol* 1996; 270:C794-802.
17. Chang Y, Ceacareanu B, Dixit M, Sreejayan N, Hassid A. Nitric oxide-induced motility in aortic smooth muscle cells: Role of protein tyrosine phosphatase SHP-2 and GTP-binding protein Rho. *Circ Res* 2002; 91:390-7.
18. Kevil CG, Orr AW, Langston W, Mickett K, Murphy-Ullrich J, Patel RP, Kucic DF, Bullard DC. Intercellular adhesion molecule-1 (ICAM-1) regulates endothelial cell motility through a nitric oxide-dependent pathway. *J Biol Chem* 2004; 279:19230-8.
19. Rhoads JM, Chen W, Gookin J, Wu GY, Fu Q, Blikslager AT, Rippe RA, Argenzio RA, Cance WG, Weaver EM, Romer LH. Arginine stimulates intestinal cell migration through a focal adhesion kinase dependent mechanism. *Gut* 2004; 53:514-22.
20. Stasiv Y, Regulski M, Kuzin B, Tully T, Enikolopov G. The *Drosophila* nitric-oxide synthase gene (dNOS) encodes a family of proteins that can modulate NOS activity by acting as dominant negative regulators. *J Biol Chem* 2001; 276:42241-51.
21. Sambrook J, Russell DW. *Molecular cloning: A laboratory manual*. Cold Spring Harbor, NY: Cold Spring Harbor Laboratory Press, 2001.
22. Nieuwkoop PD, Faber J. *Normal table of Xenopus laevis (Daudin) a systematical and chronological survey of the development from the fertilized egg till the end of metamorphosis*. Amsterdam: North-Holland, 1967.
23. Sive HL, Grainger RM, Harland RM. *Early development of Xenopus laevis: A laboratory manual*. Cold Spring Harbor, NY: Cold Spring Harbor Laboratory Press, 2000.
24. Yamaguchi Y, Katoh H, Yasui H, Mori K, Negishi M. RhoA inhibits the nerve growth factor-induced Rac1 activation through Rho-associated kinase-dependent pathway. *J Biol Chem* 2001; 276:18977-83.
25. Jaffrey SR, Erdjument-Bromage H, Ferris CD, Tempst P, Snyder SH. Protein S-nitrosylation: A physiological signal for neuronal nitric oxide. *Nat Cell Biol* 2001; 3:193-7.
26. Lee CM, Robinson LJ, Michel T. Oligomerization of endothelial nitric oxide synthase: Evidence for a dominant negative effect of truncation mutants. *J Biol Chem* 1995; 270:27403-6.
27. Stasiv Y, Kuzin B, Regulski M, Tully T, Enikolopov G. Regulation of multimers via truncated isoforms: A novel mechanism to control nitric-oxide signaling. *Genes Dev* 2004; 18:1812-23.
28. Wallingford JB, Habas R. The developmental biology of Dishevelled: An enigmatic protein governing cell fate and cell polarity. *Development* 2005; 132:4421-36.
29. Saka Y, Smith JC. Spatial and temporal patterns of cell division during early *Xenopus embryogenesis*. *Dev Biol* 2001; 229:307-18.
30. Peunova N, Enikolopov G. Nitric oxide triggers a switch to growth arrest during differentiation of neuronal cells. *Nature* 1995; 375:68-73.
31. Harris WA, Hartenstein V. Neuronal determination without cell division in *Xenopus embryos*. *Neuron* 1991; 6:499-515.
32. Wunnenberg-Stapleton K, Blitz IL, Hashimoto C, Cho KW. Involvement of the small GTPases XRhoA and XRnd1 in cell adhesion and head formation in early *Xenopus* development. *Development* 1999; 126:5339-51.
33. Habas R, Kato Y, He X. Wnt/Frizzled activation of Rho regulates vertebrate gastrulation and requires a novel Formin homology protein Daam1. *Cell* 2001; 107:843-54.
34. Tahinci E, Symes K. Distinct functions of Rho and Rac are required for convergent extension during *Xenopus* gastrulation. *Dev Biol* 2003; 259:318-35.
35. Chitaley K, Webb RC. Nitric oxide induces dilation of rat aorta via inhibition of rho-kinase signaling. *Hypertension* 2002; 39:438-42.
36. Mills TM, Chitaley K, Lewis RW, Webb RC. Nitric oxide inhibits RhoA/Rho-kinase signaling to cause penile erection. *Eur J Pharmacol* 2002; 439:173-4.
37. Sandu OA, Iro M, Begum N. Selected contribution: Insulin utilizes NO/cGMP pathway to activate myosin phosphatase via Rho inhibition in vascular smooth muscle. *J Appl Physiol* 2001; 91:1475-82.
38. Zuckerbraun BS, Stoyanovsky DA, Sengupta R, Shapiro RA, Ozanich BA, Rao J, Barbato JE, Tzeng E. Nitric oxide-induced inhibition of smooth muscle cell proliferation involves S-nitrosation and inactivation of RhoA. *Am J Physiol Cell Physiol* 2006.
39. Ellerbroek SM, Wennerberg K, Burrige K. Serine phosphorylation negatively regulates RhoA in vivo. *J Biol Chem* 2003; 278:19023-31.
40. Hess DT, Matsumoto A, Kim SO, Marshall HE, Stamler JS. Protein S-nitrosylation: Purview and parameters. *Nat Rev Mol Cell Biol* 2005; 6:150-66.
41. Tanaka H, Yamashita T, Asada M, Mizutani S, Yoshikawa H, Tohyama M. Cytoplasmic p21(Cip1/WAF1) regulates neurite remodeling by inhibiting Rho-kinase activity. *J Cell Biol* 2002; 158:321-9.
42. Lee S, Helfman DM. Cytoplasmic p21Cip1 is involved in Ras-induced inhibition of the ROCK/LIMK/cofilin pathway. *J Biol Chem* 2004; 279:1885-91.
43. Park TJ, Gray RS, Sato A, Habas R, Wallingford JB. Subcellular localization and signaling properties of Dishevelled in developing vertebrate embryos. *Curr Biol* 2005; 15:1039-44.
44. Simons M, Gloy J, Ganner A, Bullerkotte A, Bashkurov M, Kronig C, Schermer B, Benzing T, Cabello OA, Jenny A, Mlodzik M, Polok B, Driever W, Obara T, Walz G. Inversin, the gene product mutated in nephronophthisis type II, functions as a molecular switch between Wnt signaling pathways. *Nat Genet* 2005; 37:537-43.